6.2. Chirp and ELAC sediment echograph profiling

(F. Niessen, K. Dittmers)

During cruise BP01 sediment echosounding was carried out using two different systems (Tab. 6.2):

1. The hull-mount echograph ELAC was set to an operating frequency of 12 kHz and was in operation during 24 h per day along all cruise lines in the area of investigation.
2. In addition to the ELAC a portable chirp system was used along selected lines. Transducers and underwater electronics are mounted in a catamaran towed by the vessel and are connected via deck cable to the control unit in the rear laboratory. The chirp frequency range was set to 2-8 kHz.

For both ELAC and GeoChirp signal output was improved by set of mobile system components which were hooked up in the rear laboratory of the vessel. These components are parts of the mobile sediment echosounding system of AWI. Previous results from the AWI Chirp system were described from arctic lakes (Hubberten et al. 1995, Niessen et al. 1999).

On RV Boris Petrov the system was connected as illustrated in Figure 6.3 and listed in Table 6.2. Amplification, filtering, data storage (analog), digitising including import of navigation data, processing and high quality on-line plus replay printing was carried out. The system has its own GPS antenna (during BP01 placed on a container on the helicopter deck of RV Boris Petrov), amplifier and receiver. Along cruise lines, where only the ELAC system was in operation, system trigger and signal output ports (pre-amplified by the hull-mount ELAC unit in the control room behind the bridge according to Table 6.2) were connected via the ship-wiring-system into the portable AWI-system in the rear laboratory (Fig. 6.3). In comparison to the use of the ELAC system on previous cruises of RV Boris Petrov (Stein & Stepanets 2000, 2001) this new configuration had the following advantages:

1. fast availability of sediment-echosounding information in the main working laboratory
2. screen-display of both GPS positions and ELAC subbottom information on-line without time lag
3. printing GPS positions and time on subbottom analog profiles in one-minute intervals for improving station selection
4. enhancement of geological information in acoustic subbottom images by selective signal amplification, filtering and processing (stack)
5. flexible (scale, contrast) high-quality printing of subbottom profiles on two line-scan recorders
6. simultaneous noise-less analog tape storage (DAT) of trigger, signal and GPS data
7. full data replay on demand

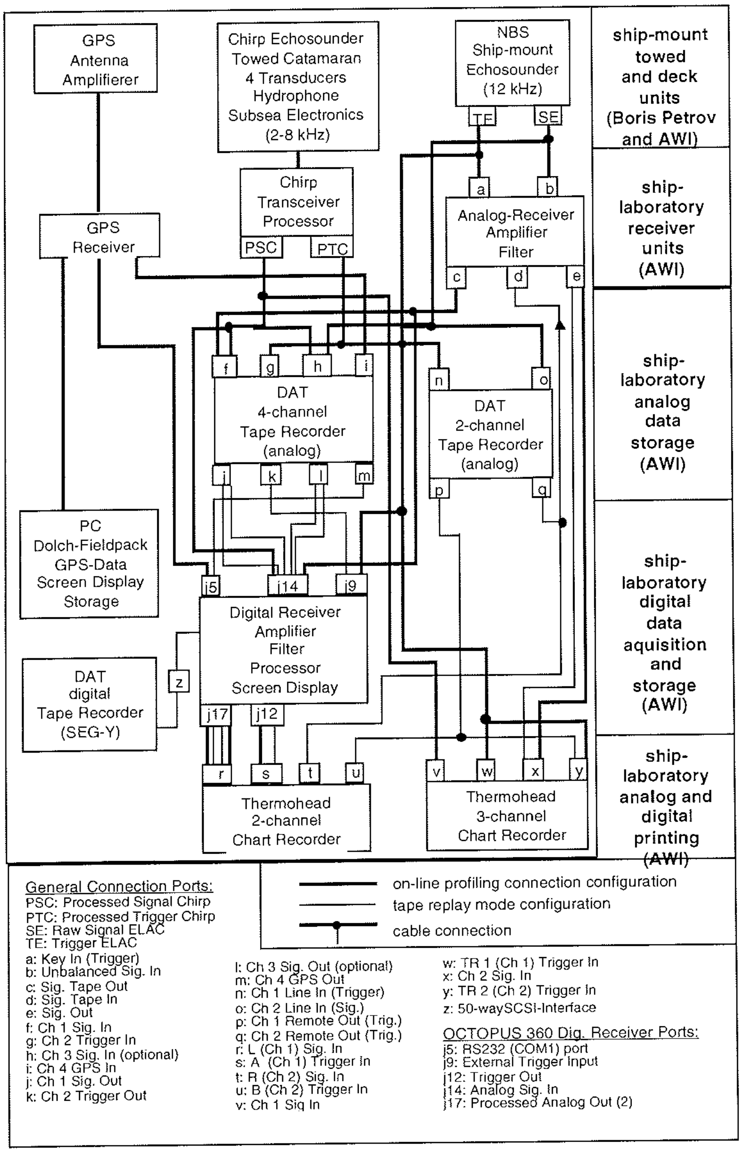

Figure 6.3: Connection diagram of different system components of the high-resolution sediment echosound systems used during BP01. For technical details of the individual components see Tab. 6.3.

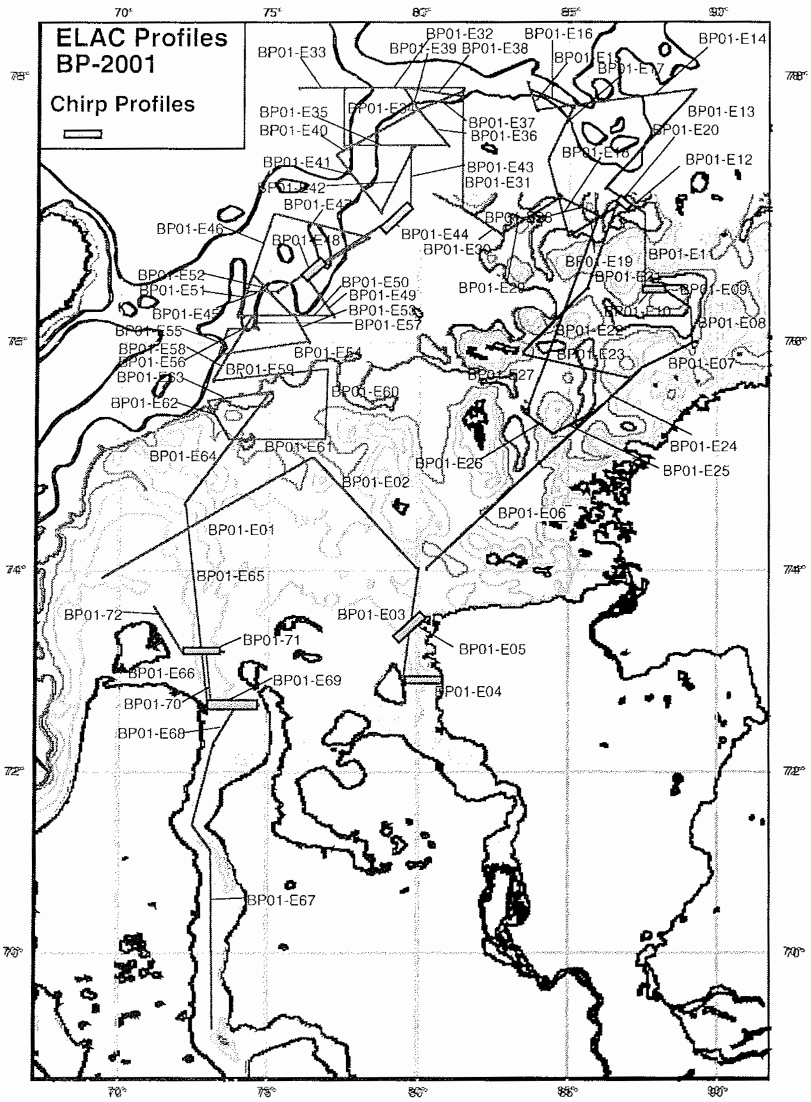

Figure 6.4: Map of ELAC and Chirp profiles recorded during BP01.

Unfortunately the DAT digital tape recorder for storing individual seismic traces in SEG-Y format (Fig. 6.3) failed shortly after the beginning of the data acquisition and could not be repaired on board. Along those lines, where the GeoChirp system was used in addition to the ELAC system, chirp trigger and signal were given a higher priority and connected with the GPS, 4-channel DAT recorder and digital receiver. In this mode, ELAC signal and trigger were stored on a 2-channel DAT-recorder simultaneously with the 4-channel data storage of the chirp (Fig. 6.3). As a result of the stable good weather and calm sea during almost the entire cruise we did not apply heave filtering to the data. Two-way travel times in seismic images are converted to meter using a sound velocity of 1500 m/s.

Tab. 6.2: Technical specifications of sediment echosound system components used during BP01.

Component (Fig.1)	Model	Manufacturer Country	Settings
NBS-Echosounder	ELAC-LAZ 72	Honeywell-Nautic Germany	Pulse: 12 kHz, level 3 Amplification: 11 (max) Range: I (0-200) 100x1
Chirp-Echosounder	GeoChirp	GeoAcoustics UK	Mode: High Penetration Trigger: 4:1 (<100m) Trigger: 2:1 (>100m)
Analog Receiver	5210	GeoAcoustics UK	Filter: 3-15 kHz Gain: 20 + 24 dB, 0 dB input Tape Output: filtered
DAT Recorder 4-Channel	PC204Ax	Sony Japan	Amplification: CH1-4: 0.5-5-5-5 Speed: normal
DAT Recorder 2-Channel	Walkman	Aiwa Japan	Speed: normal
Digital Receiver	360	Octopus UK	Sample Rate: 24 kHz Initial Gain: x10 Filter: 3.5-9.98 kHz
Chart Recorder 2-Channel	Waverly 3710	Dowty UK	Sweep: 150 or 300 ms Grid-Line-Spacing: 15 ms (10 m)
Chart Recorder 3-Channel	120-138	Ultra UK	Sweep: 150 or 300 ms Grid-Line-Spacing: 15 ms (10 m)

In total of 5200 km of ELAC profiles were recorded along 72 lines (Fig. 6.4, Tab. 6.3). In addition 8 chirp profiles with a total length of about 144 km were recorded for more detailed analysis of different acoustic facies and stratigraphy within the area of investigation (Fig. 6.4, Tab.6.3). The objectives are two-fold: (I) to search for evidence of glaciation in the Kara Sea during the last glacial maximum (LGM, marine isotope stage 2), and, (ii) to trace paleoriver channels on the open Kara shelf and to study the glacial and post glacial depositional history with respect to Siberian river runoff. These studies will be part of PhD thesis (K. Dittmers) currently carried out at AWI.

The different acoustic character of the chirp and ELAC systems are compared along a W-E line across the outer part of the Yenesei Estuary (Fig. 6.5, see also Stein & Stepanets 2000). Along this profile the total sound penetrations of both systems are almost similar and limited by a strong basal reflector located at about 16 m subbottom in the centre of the acoustic images (Fig. 6.5). Above the basal reflector, the Chirp profile is differentiated by numerous distinct reflectors whereas the ELAC image appears more diffuse. Some stratification is defined by different ELAC acoustic backscatter of the upper and lower half of the sediments overlying the base reflector, respectively. The acoustic facies of relatively thick muds associated with channel-overbank morphologies (Fig. 6.5) is typical for the outer areas of the Ob and Yenesei estuaries.

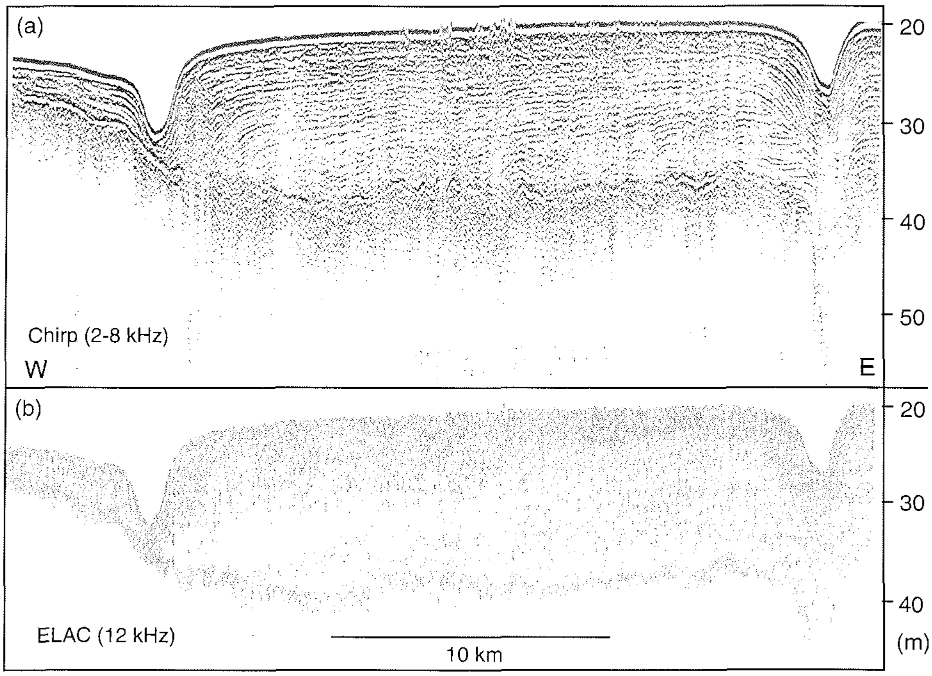

Figure 6.5: Comparison of Chirp (a) and ELAC (b) sediment echosound profiles from the Yenisei estuary. Note that both profiles were recorded simultanously. Profile no. BP-C01 (a) and BP-E04 (b), start and end positions in Tab.6.3.

Based on both relief and acoustic penetration/resolution different types of acoustic facies are identified in the inner and middle shelf areas under investigation. In ELAC images the north-west area is characterised by hummocky morphologies superimposed on several major subbottom ridges and furrows (Fig. 6.6). Sea floor backscatter is high and undifferentiated sediment penetration restricted to a few meters in general. A preliminary ship-board interpretation suggests that the relief has been formed by advances and retreats of a LGM Barents-Kara Sea ice sheet. The eastern boundary of this north-western facies forms a relatively sharp line which can be mapped (Stein et al. submitted). Furthermore, in places of this north-western acoustic facies, sediment penetration can increase up to 20 m above the strong reflector observed in this area (Fig. 6.7). These sediment complexes appear well stratified, are of limited width (on the order of 5 km) and associated with channel-overbank morphologies somehow similar to sediments found in the outer Ob and Yenesei estuaries (Fig. 6.5). The fact that these sediment complexes overly formerly glaciated terrain implies deposition after deglaciation. A possible association of these sediment complexes with early Holocene Siberian river runoff will be investigated by AWI in more detail.

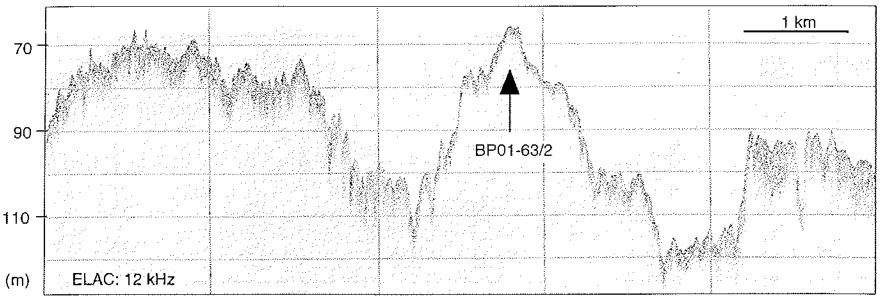

Figure 6.6: Section of ELAC profile BP-E50 between 76°12N, 74°39.8E (left: 03.09.01, 01:15UTC) and 76°12N, 74°21.2E (right: 03.09.01, 01:40UTC) as typical example of the north-western facies. Arrow marks location of core BP01-63/2.

In contrast to the north-western facies, the central and south-eastern acoustic facies is characterised by smooth relief. The relatively flat sea floor is cut by several wide channels or paleovalleys (Fig. 6.8). Acoustic penetration is usually minor associated with strong backscatter and lack of stratification. Within the channels or valleys the penetrated sediment cover is on the order of 10 m exhibiting several weak reflectors (Fig. 6.8).

In the north-eastern area of investigation the sea floor bathymetry is more variable showing deeper water associated with wider depressions separated by ridges. In depressions an additional acoustic facies is observed which is characterised by deep sound penetration and well stratified records comprising numerous distinct reflectors. In ELAC acoustic images penetration can be more than 25 m. Often the top 5 m of the sequences show higher backscatter whereas the lower part of the sequence is more transparent intercalated with thin but distinct sub-parallel reflectors (Fig. 6.9). In greater sediment depth reflections become very weak and no typical basal reflector is visible in this facies. In a chirp profile from this area (Fig. 6.10) reflectors can be observed to a sediment depth of approximately 60 m. Below this depth backscatter becomes too weak to interpret the record. Also, no distinct basal reflector is notable in chirp images in the deepest areas of these depressions. In contrast to the distinct sub-parallel reflectors in the lower sequence, the top layer is acoustically transparent and more variable in thickness from about 8 m to only a few cm in places (Fig. 6.10).

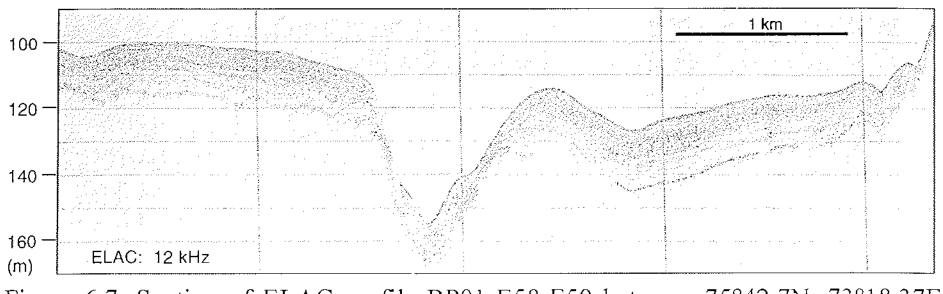

Figure 6.7: Section of ELAC profile BP01-E58-E59 between 75°42.7N, 73°18.37E (left: 04.09.01, 16:50UTC) and 75°40.08N, 73°15.2E (right: 04.09.01, 17:10UTC) as typical example of channel-overbank complexes overlying north-western facies.

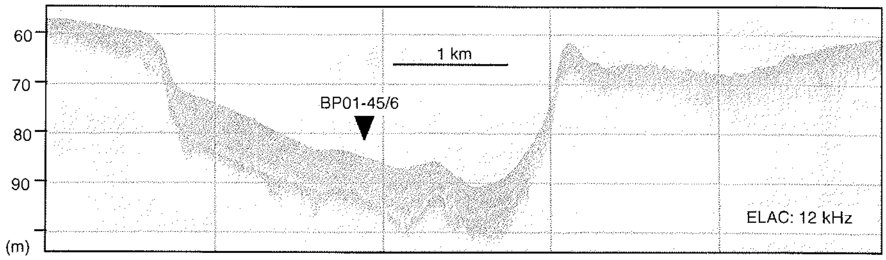

Figure 6.8: Section of ELAC profile BP01-E17 between 77°09N, 84°41.4E (left: 26.08.01, 22:48UTC) and 77°04.4N, 84°45E (right: 27.08.01, 23:12UTC) as typical example of the south-eastern facies.

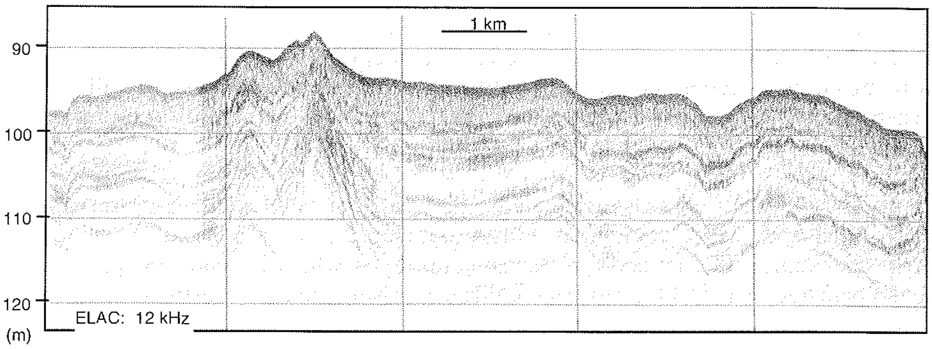

Fig. 6.9: Section of ELAC profile BP01-E11 between 77°21N, 86°57E (left: 25.08.01, 01:40UTC) and 77°24.8N, 87°14.1E (right: 25.08.01, 02:05UTC) as typical example of the north-eastern facies.

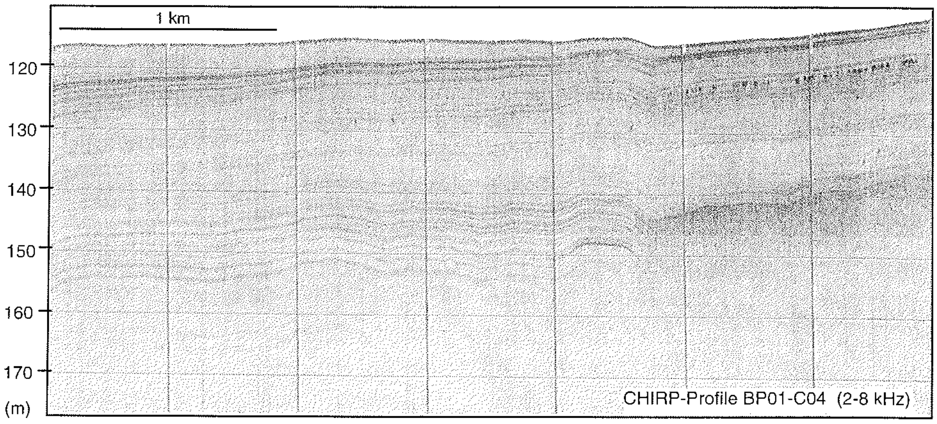

Figure 6.10: Section of Chirp profile BP01-C04 between 77°05.2N, 86°55.8E (left: 27.08.01, 23:45UTC) and 77°06.4N, 86°47.5E (right: 27.08.01, 23:58UTC) as typical example of the north-western facies.

Tab. 6.3: List of ELAC and Chirp profiles recorded during BP01

Date	Number	Beginning		End		Direction	Remarks
		Latitude (N)	Longitude (E)	Latitude (N)	Longitude (E)		
14.08.	BP01-E01	73°55′	69°30′	75°	76°30′	SW-NE	BP01-01
14./15.08.	BP01-E02	75°	76°30′	74° 0.3′	80°0.45′	NW-SE	BP01-01, -02
15.08.	BP01-E03	74° 0.3′	80°0.45′	72°56′	79°35′	NNE-SSW	
15.08.	BP01-E04	72°56′	79°35′	72°56′	80°45.2′	W-E	BP01-03, BP99-08, BP99-09; Chirp Profile BP01-C01
22.08.	BP01-E05	73°20′	79°23′	73°32.6′	80°08′	SW-NE	BP01-25/BP99-04, BP99-05, BP00-23; Chirp Profile BP01-C02
23./24.08.	BP01-E06	74°0.07′	80°19.87′	75°46′	87°28′	SW-NE	BP01-41, -42, -43
24.08.	BP01-E07	75°46′	87°28′	75°59′	89°23′	mix	BP01-28
24.08.	BP01-E08	75°56.4′	89°15.9′	76°16.03′	89°07.69′	SSE-NNW	BP01-28, -29
24.08.	BP01-E09	76°16.03′	89°07.69′	76°24.75′	88°10.76′	SE-NW	BP01-29, -30
24.08.	BP01-E10	76°24.7′	88°14.8′	76°24.7′	87°33′	E-W	BP01-30; Chirp Profile BP01-C03
24./25.08.	BP01-E11	76°24.7′	87°33′	77°	87°33′	S-N	
25.08.	BP01-E12	77°	87°33′	77°11′	86°15′	SE-NW	BP01-38, -39
25.08.	BP01-E13	77°11′	86°15′	77°54.29′	89°20.15′	SW-NE	BP01-31, -32, -33, -34
25.08.	BP01-E14	77°54.29′	89°20.15′	77°45′	84°	ENE-WSW	BP01-36, -37
26.08.	BP01-E15	77°45′	84°	77°57′	83°40′	SSE-NNW	BP01-35
26.08.	BP01-E16	77°54.3′	83°45.94′	77°47.1′	85°12.6′	NW-SE	BP01-35, -36
26./27.08.	BP01-E17	77°48.9′	86°12.7′	77°24.5′	84°24′	NE-SW	BP01-37
27.08.	BP01-E18	77°24.5′	84°24′	76°50′	85°	NNW-SSE	BP01-45
27.08.	BP01-E19	76°50′	85°	77°05.2′	86°55.8′	SW-NE	BP01-38, -44
27.08.	BP01-E20	77°05.2′	86°55.8′	77°06.79′	86°44.87′	SE-NW	BP01-38, -39; Chirp Profile BP01-C04
27.08.	BP01-E21	77°06.79′	86°44.87′	76°25.2′	85°39.9′	NNE-SSW	BP01-39, -40
28.08.	BP01-E22	76°25.2′	85°39.9′	75°54′	83°35′	NE-SW	BP01-40
28.08.	BP01-E23	75°54′	83°35′	75°41.35′	87°08.1′	ENE-WSW	BP01-41
28.08.	BP01-E24	75°41.35′	87°08.1′	75°23′	85°49.9′	NE-SW	BP01-41, -42, -43; part of BP01-E06

Date	Number	Beginning Latitude (N)	Longitude (E)	End Latitude (N)	Longitude (E)	Direction	Remarks
28.08.	BP01-E25	75°23′	85°49.9′	75°13′	84°33′	NE-SW	
28.08.	BP01-E26	75°13′	84°33′	75°23′	83°41′	SE-NW	BP00-32, -33, -34, -35
29.08.	BP01-E27	75°23′	83°41′	76°58.25′	86°02.2′	SSW-NNE	BP01-40, -44
29.08.	BP01-E28	76°58.23′	86°01.9′	77°06.8′	84°44′	SE-NW	BP01-44, -45
29.08.	BP01-E29	77°06.8′	84°44′	76°50′	82°50′	NE-SW	BP01-45
29.08.	BP01-E30	76°50′	82°50′	77°02′	81°30′	SE-NW	BP00-36
29.08.	BP01-E31	77°02′	81°30′	77°55′	81°30′	S-N	BP01-48, -49, -50
30.08.	BP01-E32	77°55′	81°30′	77°55′	76°	E-W	BP01-46, -47, -51
30.08.	BP01-E33	77°55′	76°	77°55′	77°30′	W-E	BP01-46, -47
30.08.	BP01-E34	77°55′	77°30′	77°30′	77°30′	N-S	BP01-47
30.08.	BP01-E35	77°30′	77°30′	77°30′	81°	W-E	BP01-52, -53, -54
31.08.	BP01-E36	77°30′	81°	77°45′	80°	SE-NW	
31.08.	BP01-E37	77°45′	80°	77°53.5′	81°30	SW-NE	BP01-48
31.08.	BP01-E38	77°50.9′	81°30′	77°54.7′	79°29.5′	ESE-WNW	BP01-50, -51
31.08.	BP01-E39	77°54.7′	79°29.5′	77°45′	80°	NW-SE	BP01-51
31.08.	BP01-E40	77°45′	80°	77°26′	77°15′	NE-SW	
01.09.	BP01-E41	77°26′	77°15′	77°	78°47′	NW-SE	
01.09.	BP01-E42	77°	78°47′	77°30′	79°52′	SW-NE	BP01-52
01.09.	BP01-E43	77°30′	79°46.2′	77°03′	79°44′	N-S	BP01-54, -55
01.09.	BP01-E44	77°03′	79°44′	76°23′	75°20′	NE-SW	BP01-55; Chirp Profile BP01-C05
02.09.	BP01-E45	76°23′	75°20′	76°23′	74°20′	E-W	BP01-60
02.09.	BP01-E46	76°23′	74°20′	76°59.6′	75°10.3′	SW-NE	BP01-56, -59
02.09.	BP01-E47	76°59.6′	75°10.3′	76°48.1′	78°21.2′	WNW-ESE	BP01-56, -57, -58
02.09.	BP01-E48	76°48.1′	78°21.2′	76°31.7′	76°16.4′	NE-SW	BP01-58; Chirp Profile BP01-C05
02.09.	BP01-E49	76°31.7′	76°16.4′	76°12′	77°12′	NW-SE	

Date	Number	Beginning Latitude (N)	Beginning Longitude (E)	End Latitude (N)	End Longitude (E)	Direction	Remarks
03.09.	BP01-E50	76°12′	77°12′	76°12′	74°	E-W	BP01-61, -62, -63
03.09.	BP01-E51	76°12′	74°	76°31.2′	74°31′	SW-NE	BP01-59
03.09.	BP01-E52	76°31.2′	74°31′	76°12.1′	75°45.3′	NW-SE	BP01-59, -60, -61
03.09.	BP01-E53	76°12.9′	75°53.1′	75°59′	76°22′	NW-SE	BP01-61
04.09.	BP01-E54	75°59′	76°22′	75°53′	73°28′	ENE-WSW	BP01-64
04.09.	BP01-E55	75°53′	73°28′	76°05′	73°42′	SSW-NNE	
04.09.	BP01-E56	76°05′	73°42′	76°05′	74°42′	W-E	
04.09.	BP01-E57	76°05′	74°42′	76°12′	74°12′	SE-NW	BP01-62
04.09.	BP01-E58	76°12′	74°29.3′	75°40′	73°12′	NE-SW	BP01-63, -64
05.09.	BP01-E59	75°40′	73°12′	75°45′	77°	WSW-ENE	BP01-65
05.09.	BP01-E60	75°43′	75°50.8′	75°10′	76°55.1′	NW-SE	BP01-65, -66
05.09.	BP01-E61	75°10′	76°55.1′	75°10′	73°46′	E-W	BP01-66
06.09.	BP01-E62	75°10′	73°46′	75°30′	73°02′	SE-NW	
06.09.	BP01-E63	75°30′	73°02′	75°34′	75°10′	WSW-ENE	
06.09.	BP01-E64	75°34′	75°10′	74°35′	72°15′	NE-SW	BP01-67, -68
06.09.	BP01-E65	74°35′	72°15′	72°40′	73°05′	NNW-SSE	BP01-68
07.09.	BP01-E66	72°40′	73°05′	72°40′	74°45′	W-E	BP01-69, -70, -71
09./10.09.	BP01-E67	69°03.3′	73°13.7′	72°15′	73°15′	general S-N	BP01-79, -80
	BP01-E68	72°15′	73°15.2′	72°40′	74°05′	SW-NE	BP01-80, -81
	BP01-E69	72°40′	74°05′	72°40′	73°10′	E-W	BP-01-70, -71; Chirp BP01-C07
	BP01-70	72°40′	73°10′	73°11.8′	73°01.7′	S-N	BP01-82
	BP01-71	73°12′	73°33′	73°12′	72°10′	E-W	BP01-82, -83; Chirp BP01-C08
	BP01-72	73°12′	72°10′	73°35^	72°	SSE-NNW	